Waste Management 114 (2020) 225–233

Contents lists available at ScienceDirect

Waste Management

journal homepage: www.elsevier.com/locate/wasman

Catalytic co-pyrolysis of sewage sludge and rice husk over biochar catalyst: Bio-oil upgrading and catalytic mechanism

Zhenzi Qiu [a,b], Yunbo Zhai [a,b,*], Shanhong Li [a,b], Xiangmin Liu [a,b], Xiaoping Liu [a,b], Bei Wang [a,b], Yali Liu [a,b], Caiting Li [a,b], Yanjun Hu [c]

[a] College of Environmental Science and Engineering, Hunan University, Changsha 410082, PR China
[b] Key Laboratory of Environmental Biology and Pollution Control (Hunan University), Ministry of Education, Changsha 410082, PR China
[c] Department of Technical Centre, Hunan Sheng Provincial Quality Supervision and Inspection Institute, Changsha 410007, PR China

ARTICLE INFO

Article history:
Received 13 May 2020
Revised 22 June 2020
Accepted 6 July 2020

Keywords:
Catalytic co-pyrolysis
Sewage sludge
Rice husk
Biochar catalyst
Bio-oil

ABSTRACT

In this study, the effects of different biochar catalysts on the quality of bio-oil derived from the co-pyrolysis of sewage sludge (SS) and rice husk (RH) are explored. Catalysts include SS biochar (SWC), RH biochar (RHC), mixed SS and RH biochar (SRC), and RH ash (RHA). The quality of bio-oil was evaluated based on the results of gas chromatography-mass spectrometry (GC–MS; including the contents of hydrocarbons and N-species), oxygen content, higher heating value, and pH. The GC–MS analysis results illustrated that N-species content in the bio-oil reduced with the addition of the biochar catalyst, while the hydrocarbons content increased from 15.51% for co-pyrolysis to 38.74–61.84% for different biochar catalysts at a catalytic temperature of 650 °C. RHC exhibited the best catalytic effect in terms of decreasing the content of N-species by 58.79% and increasing the content of hydrocarbons by nearly four times compared to co-pyrolysis. The higher heating value of bio-oil raised from 25.75 to 34.67 MJ/kg, while oxygen content decreased from 31.1 to 8.81 wt%, and the pH increased from 4.06 to 5.48. Moreover, the catalytic mechanism of catalytic co-pyrolysis over RHC, including the hydrocarbon generation pathway and nitrogen removal, is also discussed here. High specific surface area of RHC provides sufficient active sites (e.g. O-containing and N-containing functional groups) for the catalytic reaction of pyrolytic intermediates.

1. Introduction

Sewage sludge (SS) is a semi-residual solid produced by sewage treatment that contains many organic substances, heavy metals, and pathogenic bacteria (Fonts et al., 2012; Liu et al., 2020). As the amount of SS increasing annually, its treatment has received widespread attention (Peng et al., 2017). Pyrolysis is a promising pathway for SS treatment, as it can not only effectively reduce the volume of SS, but also convert organic matter into different available energy forms, such as bio-oil, biochar, and gas (Syed-Hassan et al., 2017). However, the individual pyrolysis of SS has some drawbacks, including low energy efficiency, and high bio-oil nitrogen content (Wang et al., 2019). Co-pyrolysis of SS with biomass is an effective method of resolving these issues as it has significant synergetic effects that can effectively improve the composition of bio-oil (Alvarez et al., 2015). Rice husk (RH) is an ideal raw material for pyrolysis on account of its high content of volatiles, large available volume as well as low cost (Naqvi et al., 2016; Tsai et al., 2007). Some researchers have investigated the interactions in the co-pyrolysis of SS and RH. For example, (Naqvi et al., 2019) studied the synergistic effect of the co-pyrolysis of SS and RH via thermogravimetric analysis, and found that co-pyrolysis can more efficiently recover organic components. (Zhang et al., 2015) found that co-pyrolysis can increase the syngas yield and improve its lower heating value. (Wang et al., 2019) studied the effect of co-pyrolysis on gas and biochar product, and found that co-pyrolysis can promote the production of CO_2 and improve the specific surface area of biochar. However, few studies discussed bio-oil through the co-pyrolysis of SS and RH. Therefore, this study explored the characteristics of bio-oil produced through SS and RH co-pyrolysis. However, different raw materials mix and pyrolyze in a certain proportion, which is still hard to produce high-quality fuel products. The higher heating value (HHV) of bio-oil during the co-pyrolysis of SS and 15% poplar sawdust was 27.5 MJ/kg (Zuo et al., 2014), which is well below that of commercial liquid fuels (45–46 MJ/kg) (Fonts et al., 2012). Pyrolytic bio-oil contains many oxygen-containing (O-containing) compounds, resulting in

* Corresponding author.
E-mail address: ybzhai@hnu.edu.cn (Y. Zhai).

https://doi.org/10.1016/j.wasman.2020.07.013
0956-053X/

issues such as high viscosity, low heating value, and high acidity (Wang et al., 2017a). Therefore, it is important to introduce a step to further improve the usability of bio-oil.

Compared with conventional pyrolysis, the integration of catalyst into pyrolysis can effectively upgrade the quality of bio-oil. During catalytic pyrolysis, the pyrolytic intermediates contact with the catalyst and further diffuse into cavities to react with the active sites on the catalyst, thereby promoting oxygen removal via decarboxylation, decarbonylation, and dehydration reactions (Yildiz et al., 2015). Currently, many studies conducted on catalysts have focused on zeolite catalysts, inorganic salts, and metal oxides. However, these catalysts are expensive or easily deactivated, which greatly limits their large-scale use in industry (Zhang et al., 2014a).

To reduce costs and avoid carbon deposition, biochar has begun to attract attention as a low-cost, effective catalyst. As it is naturally generated during the gasification/pyrolysis process, the use of biochar as a catalyst can reduce potential waste disposal costs, thereby increasing its added-value (e.g. phenols and hydrocarbons) (Buentello-Montoya et al., 2019; Duan et al., 2019). (Zhao et al., 2018) found that the catalytic performance of straw char was better than that of lignite char due to the excellent chemical structure of straw char. Therefore, the catalytic effects of different types of biochar vary widely. (Shen et al., 2014) investigated the conversion of bio-oil over the RH biochar (RHC)-supported nickel–iron catalysts, while (Daorattanachai et al., 2018) used SW biochar (SWC)-supported Re-Ni bimetallic catalyst for the cracking/reforming of biomass bio-oil. Generally, the catalytic activity of biochar mainly depends on the pore structure (Wang et al., 2019), alkali metals and alkaline earth metals, functional groups, and adsorption (Chen et al., 2018, 2020). Fu et al. (2018) investigated the catalytic pyrolysis of coal using char-based catalysts and found that the light tar increased by 30.31% from that obtained by coal pyrolysis alone due to the abounding active sites (e.g. alkali metals and functional groups) on the biochar. Chen et al. (2020) introduced N-doped biochar to bamboo pyrolysis, and found that it could accelerate generation of aromatic hydrocarbons and inhibit the formation of the O-containing compounds through abounding O-containing functional groups on the catalyst. However, the mechanism of pyrolysis with biochar catalyst for bio-oil upgrading is unclear.

In this study, we propose a green and effective method for bio-oil upgrading by adding four biochar catalysts (including SWC, mixed SS and RH biochar (SRC), RHC, and RH ash (RHA)) to the co-pyrolysis of SS and RH. To compare the performances of different catalysts, the quality of obtained bio-oil was analyzed by the gas chromatography-mass spectrometry (GC–MS) and elemental analysis. Furthermore, the possible catalytic mechanism, including the hydrocarbons generation pathway and nitrogen removal, was proposed by discussing the physical and chemical properties of RHC.

2. Materials and methods

2.1. Samples and catalysts preparations

SS and RH came from a wastewater treatment plant and rice mill in Changsha, Hunan Province, China, respectively. The feedstocks were dried at 105 °C for 24 h, and grinded into powder (150–250 μm in diameter) before conducting the experiments. The SS and RH were then mixed uniformly at a weight ratio of 1:1 for the co-pyrolysis experiments.

The characteristics of the raw materials are listed in Table A1. Proximate analysis was conducted following the method for solid biofuel analysis in China (Chinese Standard Methods, GB/T 28731-2012), and the fixed carbon content was calculated by subtracting the sum of the volatile, ash, and moisture contents from the 100%. Ultimate analysis (including oxygen, carbon, hydrogen, sulfur, and nitrogen) was conducted using an elementary analyzer (Vario Micro Cube), while the alkali and alkaline earth metals (AAEMs) were determined using an inductively coupled plasma-mass spectroscopy (ICP-MS, Agilent 7900, Japan). RH has lower ash (12.77 wt%) and higher volatile (63.74 wt%) contents than SS, indicating that the addition of RH could release more volatile components. Additionally, the content of nitrogen (0.34 wt%) of RH is much lower than that of SS (2.99 wt%) as SS containing large proteins.

RHC catalyst was derived from RH pyrolysis. RH was placed in a tube furnace for pyrolysis under a nitrogen atmosphere, and the pyrolysis temperature was set to 850 °C, which was held for 30 min. In the same way, SWC and SRC were obtained from the pyrolysis of SW and co-pyrolysis of SW and RH, respectively. Finally, RHA was obtained by calcining RHC in air at 850 °C.

2.2. Pyrolysis experiment procedure

The pyrolysis experiments were placed in a two-stage tube furnace with a quartz tube of 78 mm in inner diameter and 1200 mm in length, as shown in Fig. S1. The device was divided into two zones, i.e., the first reaction zone and second reaction zone. During the co-pyrolysis experiment performed at 550 °C, 6 g sample was placed in the first reaction zone. In the catalytic co-pyrolysis experiment, 6 g sample was put in the first reaction zone, and 2 g catalyst was placed in the second reaction zone. The temperature of the first and second reaction zone was controlled at 550 and 650 °C, respectively. Before the experiment, the sample or catalyst was added and the nitrogen gas flow was kept at least half an hour to ensure that atmosphere was oxygen-free during the pyrolysis experiment. When the temperature of the second reaction zone reached 650 °C, the first reaction zone was heated from 30 to 550 °C at a steady heating rate of 10 °C/min, which was held for 30 min. Accordingly, the co-pyrolysis experiments subjected to different catalysts were denoted as SWC, SRC, RHC, and RHA, respectively. A control group without catalyst was set and denoted as thermal. The condensable components named as bio-oil were collected using a condensing system consisting of three gas cylinders filled with acetone placed in an ice-water bath. When the device temperature dropped to 30 °C, solid products were collected, denoted as biochar. The yields of bio-oil and biochar reflected the proportion of product mass in the raw materials, and the gas yield was calculated by determining the mass balance. Two repeat runs were carried out under the same conditions to ensure the repeatability of each experiment.

2.3. Characterization

The chemical compositions of bio-oil were determined through GC–MS (QP2010, SHIMADZU, HP-5MS capillary column) under a helium atmosphere. The column oven temperature was initially held at 40 °C for 2 min, and then heated to 160 °C at a rate of 6 °C/min, and it was heated to 280 °C at a heating rate of 4 °C/min for 6 min in the end. The element contents (including carbon, hydrogen, sulfur, and nitrogen) of the bio-oil were identified using an elementary analyzer (Vario Micro Cube), and the oxygen content was calculated by subtracting the sum of the carbon, hydrogen, sulfur, and nitrogen contents from 100%. The pH value was determined using a pH meter (PHS-25).

An automatic gas adsorption analyzer (ASAP 2020 PLUS, Micromeritics, USA) was used to determine the pore characteristics of the catalysts. The surface characteristics and structure of the catalyst was determined through scanning electron microscopy (SEM, TESCAN MIRA3 LMH). The surficial functional groups of the cata-

lysts were analyzed using X-ray photoelectron spectroscopy (XPS, EscaLab Xi+, USA) with an Al Kα (12.5 kV, 16 mA) radiation source. The curves on the C1s, O1s, and N1s peaks were fitted by XPS peak4.0.

3. Results and discussions

3.1. Physicochemical properties of catalysts

3.1.1. Morphological analysis

To understand the surface structure of the catalysts, their micromorphology was examined using SEM. As shown in Fig. S2, the surface of SWC was rough with particles of different shapes, and did not exhibit porous structure. However, the pore structure of RHC could be observed. This could have been due to the release of volatiles during the pyrolysis process, which destroyed the original dense structure to form an open pore structure. It was worth noting that the surface of the RHA gathered of regularly-shaped particles, which were large silica clusters that formed during air calcination. Additionally, there were irregular particles on the pores in the SRC, which was generated from SS. These SEM images indicate that RHC became a highly porous carbonaceous material after high-temperature pyrolysis. Therefore, it was more suitable for use as a catalyst than other biochar.

3.1.2. Pore analysis

The pore structure parameters of the catalysts are summarized in Table 1. The S_{BET} of RHC was 127.83 m^2/g, which was significantly higher than that of RHC derived from microwave pyrolysis (51.99 m^2/g) (Zhang et al., 2015). However, the S_{BET} of RHA was only 5.89 m^2/g, which was most likely due to the collapse of the internal pore structure of the RH during air calcination (Xu et al., 2018). Generally, S_{BET} is strongly related to the catalyst performance. A higher specific surface area is beneficial for promoting the reformation of pyrolysis intermediates, which can be ascribed to two reasons: (1) it can prolong the dwell time of volatiles during the catalytic co-pyrolysis, and (2) it provides more active sites for the catalytic reaction. The S_{BET} of SWC (38.52 m^2/g) and SRC (90.77 m^2/g) was lower than that of RHC. 3.1.3 Surface functional group

3.1.3. Surface functional group

XPS analysis was performed to observe the functional groups of the catalysts. Fig. S3 presents the fitting curves of various peaks, and the relative contents of functional groups in C1s, O1s, and N1s are summarized in Fig. 1. As can be seen from Fig. 1, the C1s spectra of catalysts were deconvoluted into three peaks, i.e., C—C (284.6 eV), C—O (286.0–286.3 eV), C=O (287.3–287.6 eV). The O1s spectra were deconvoluted into four peaks, i.e., C=O (531.0–531.9 eV), O—C=O/—OH (532.3–532.8 eV), O—C=O/C—O (533.1–533.8 eV), and —COOH (534.3–535.4 eV) (Zhou et al., 2007). The

Table 1
Specific surface area, total pore volume, and average pore diameter of different catalysts.

Catalyst	S_{BET}[a] (m^2/g)	V_t[b] (cm^3/g)	D_a[c] (nm)
SWC	38.52	0.0851	7.89
SRC	90.77	0.0961	5.81
RHC	127.83	0.0883	5.10
RHA	8.51	0.0076	4.20

[a] S_{BET} (specific surface area) was counted by Brunauer-Emmett-Teller (BET) equation.
[b] V_t (total pore volume) was generally understood to as the total volume of single point adsorption at P/P_O = 0.99.
[c] D_a (average pore diameter) was determined from the adsorption branches of the isotherms by the BJH method.

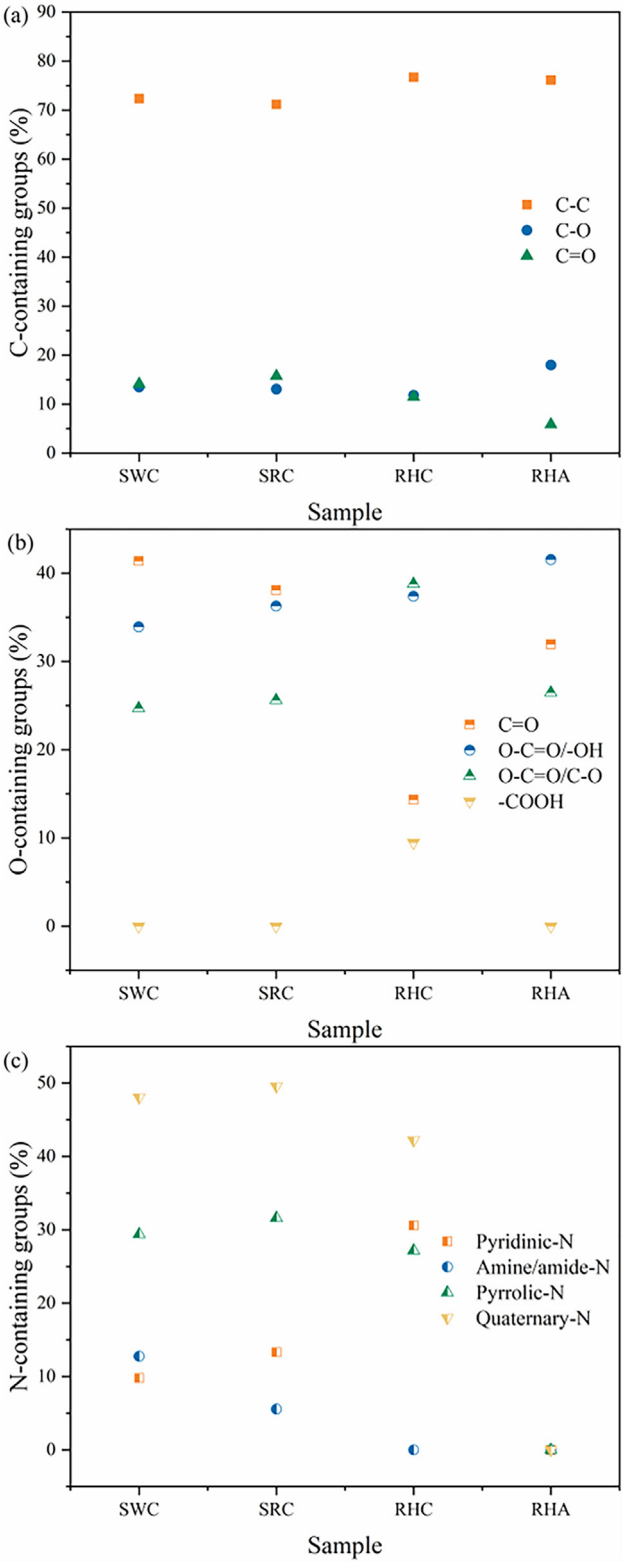

Fig. 1. The relative content of C- (a), O- (b) and N-containing (c) functional groups in biochar catalysts.

N1s spectra was deconvoluted into four peaks, i.e., pyridinic-N (398.5 ± 0.3 eV), pyrrolic-N (400.5 ± 0.3 eV), amine/amide-N (400.0 ± 0.3 eV), and quaternary-N (401.2 ± 0.3 eV) (Chen et al., 2017; Chen et al., 2018a, 2018b). It was observed that the proportion of C-C group was largest (71.19–76.72%) as high-temperature

pyrolysis exacerbates the carbonization of biochar. For O-containing functional groups, C═O, O—C═O/—OH, and O—C═O/C—O were present in SWC, SRC, and RHA, while RHC additionally contained —COOH. C═O and O—C═O/—OH were the main groups in SWC and SRC, while O—C═O/—OH and O—C═O/C—O were the main groups in RHC. Among the N-containing functional groups of biochar, quaternary-N content (42.22–48.06%) was highest, followed by pyrrolic-N or pyridinic-N. Additionally, no N-containing groups were found in RHA. The abounding O-containing and N-containing functional groups with developed pores play an important role in catalytic pyrolysis.

3.2. Catalytic co-pyrolysis of sewage sludge and rice husk

3.2.1. Effect of catalyst on distribution of products

The distribution of products from co-pyrolysis with different catalysts is shown in Table 2. It was observed that the biochar, bio-oil, and gas product yields of co-pyrolysis were 53.48 wt%, 17.21 wt%, and 29.31 wt%, respectively. For the thermal sample, the gas yield increased to 32.53 wt%, while the bio-oil yield decreased significantly by 13.95 wt%. This is because the high temperature promoted the secondary cracking of bio-oil components to form gas, leading to an increase in gas production at the expense of bio-oil reduction (Ateş and Işikdağ, 2009). With the addition of a catalyst, the gas and bio-oil yields were higher and lower than those of the thermal sample, respectively. This suggests that the introduction of a biochar catalyst leads to a reduction in bio-oil yield. The pore structure of catalysts absorbed some pyrolysis intermediates, while its abounding functional groups promoted the catalytic reaction of pyrolysis intermediates. The bio-oil (9.45 wt%) and gas (37.27 wt%) yields of RHC were lowest and highest, respectively, suggesting that RHC may have a higher catalytic performance for pyrolysis intermediates. Additionally, the yield of biochar remained stable during catalytic co-pyrolysis, as the catalyst only affected the secondary pyrolysis reactions in the gas phase.

3.2.2. Effect of catalyst on the chemical composition of bio-oil

Generally, the typical compositions of bio-oil derived from the co-pyrolysis of SS and RH can be categorized as follows: hydrocarbons, N-species, acids, esters, ketones, phenols, alcohols, furans, anhydrosugars, aldehydes, and ethers (Arazo et al., 2017; Cai et al., 2018). The chemical compositions of bio-oil were determined by GC–MS, shown in Fig. 2a. Note here that the GC–MS cannot be used for quantitative analysis. However, when the quality of different samples is constant, it can be used to compare the changes in the relative content of different chemical components (Qiang et al., 2009).

High-temperature cracking and dehydration reactions of cellulose can produce anhydrosugars (Carlson et al., 2010). However, the AAEMs present in feedstocks stimulated the cleavage of C-C bonds in the pyranose ring, rather than the cleavage of glycosidic linkages (Zhang et al., 2018). The AAEMs contents are listed in Table A1. It was observed that the anhydrosugars contents (0–1.53%) of all catalytic samples were lower than the thermal sample (2.17%). While the furans contents of all the catalytic samples (3.36–6.16%) were higher than that of the thermal sample (2.61%). This demonstrates that the biochar catalyst could encourage the conversion of anhydrosugars, which can transfer into furans through deoxygenation reactions such as dehydration and rearrangement reaction (Carlson et al., 2011).

Acids contents under co-pyrolysis reached 23.48%, and it mainly included long-chain fatty acids (e.g. oleic acid and n-hexadecanoic acid). Subsequently, it was observed that acids completely disappeared after using SWC, SRC, and RHC as catalyst. Part of the reduction in acids can be attributed to the ketization reaction, which occurred between two acid components to generate ketones, carbon dioxide, and water (Wang et al., 2017a), and was consistent with the increase of ketones content. Another reason for the reduction in acids is that long-chain fatty acids undergo various reactions (including dehydration, cyclization, decarbonylation, and aromatization) over biochar catalyst to generate hydrocarbons (Chen et al., 2018a), which was in accordance with the increase in the content of hydrocarbons. However, RHA still retained an acids content of 0.9%, which demonstrated that its catalytic effect was inferior to that of other biochar catalysts.

Phenols are mainly produced by the thermal cracking of lignin, which typically forms more easily above 500 °C (Zhang et al., 2014b). For bio-oil of co-pyrolysis, the phenols were mainly phenol, alkoxy phenols, and alkyl phenols. However, alkoxy phenols reduced significantly after the catalyst was introduced. Fig. 2a shows that the phenol contents obtained with co-pyrolysis, thermal, SWC, SRC, RHC and RHA were 16.74%, 7.35%, 10.03%, 1.87%, and 2.15%, respectively. It indicates that the presence of catalyst can boost the decomposition of phenols, and RHC has the best effect. However, some studies have found that biochar catalyst can increase phenols content, especially simple phenols (e.g. phenol, alkyl phenols) (Norouzi et al., 2016). Simple phenols are an intermediate product that can further convert to hydrocarbons by removing —OH (Ren et al., 2014). The increase in the content of hydrocarbons and decrease in phenols can be due to that biochar catalyst further converts simple phenols into monocyclic aromatic hydrocarbons after promoting the formation of simple phenols (Hu et al., 2018). (Dong et al., 2018) reported that O-containing functional groups (C═O, O—C═O/C—O) are present on the surface of biochar which can react with phenols, thereby promoting the removal of phenolic side chains. (Zhang et al., 2015) found that the presence of the biochar catalyst promotes the conversion of phenols to alkyl monoaromatics, which may be due to demethoxylation and isomerization reactions (An et al., 2020).

Hydrocarbons in bio-oil are considered as an ideal component of fuel as they can increase the heating value of fuel without generating pollutants. Fig. 2a shows that the addition of the catalyst greatly increased the hydrocarbons contents of bio-oil. Co-pyrolysis generated a small amount of hydrocarbons contents (15.51%), while the thermal and catalytic samples generated higher amounts of hydrocarbons, ranging from 26.33 to 61.84%. Especially the RHC catalyst, its hydrocarbons contents were as high as 61.84%, which was nearly four times that obtained through co-pyrolysis.

The contents of N-species obtained under co-pyrolysis, thermal, SWC, SRC, RHC, and RHA were 13.64%, 30.2%, 12.82%, 10.05%, 5.6%, and 36.51%, respectively. It was clearly seen that the N-species increased sharply after high-temperature catalysis. Additionally, the N-species were significantly reduced after being catalyzed by the biochar (including SWC, SRC, and RHC). This indicates that the biochar catalyst has a certain denitrification effect, and was

Table 2
Effect of catalyst on the distribution of the products.

Yield (wt.%)	Co-pyrolysis	Thermal	SWC	SRC	RHC	RHA
Biochar	53.48	53.52	53.49	53.67	53.28	53.10
Bio-oil	17.21	13.95	11.25	10.72	9.45	12.03
Gas	29.31	32.53	35.26	35.61	37.27	34.87

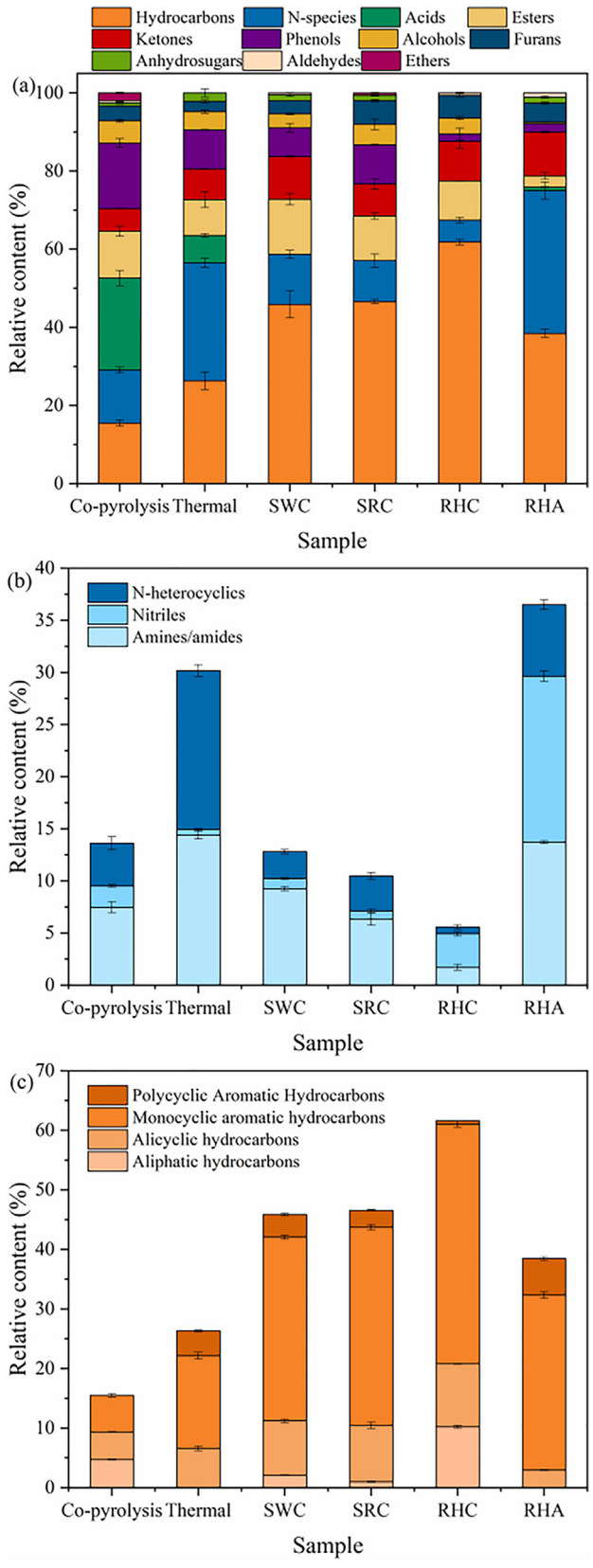

Fig. 2. Effect of catalysts on the chemical composition of bio-oil (a) N-species (b) Hydrocarbons (c).

likely to promote the decomposition of the N-species to generate NH_3/HCN or hydrocarbons, but the analysis of the gas product was not discussed here because the main goal of this study is to elucidate the influence of biochar catalyst on the bio-oil. Furthermore, it may have also boosted the reaction between the N-containing intermediates and O-containing functional groups presented on biochar catalyst.

3.2.3. Effect of catalyst on the distribution of N-species in bio-oil

The N-species can be divided into amides/amines, nitriles, and nitrogen heterocyclics (N-heterocyclics). The distribution of N-species is summarized in Fig. 2b. It was observed that the content of amides/amines and N-heterocyclics in the thermal sample were significantly higher than those under co-pyrolysis, while the content of nitriles was lower. The NH_3/NH_2* obtained from SS pyrolysis reacted with acids to form amides/amines, which corresponded to the increase in the content of amides/amines and decrease in the content of acids. (Tian et al., 2014) found that amides/amines can transform into N-heterocyclics with the simultaneous release of NH_3 during SS pyrolysis. Besides, the cyclization reaction of the other N-species (e.g. nitriles) could also generate N-heterocyclics (Chen et al., 2018b). High-temperature catalysis not only promotes the formation of amides/amines, but also boosts the conversion of N-containing intermediates into N-heterocyclics. With the addition of biochar catalyst (including SWC, SRC, and RHC), the content of amides/amines and N-heterocyclics decreased greatly, while that of nitriles content increased slightly. This is because the amides/amines react with the O-containing functional groups (including O—C=O, —COOH, and —OH) on biochar catalyst to form amine/amide-N remained on the catalyst (Chen et al., 2018b). Additionally, amides/amines may convert into aliphatic hydrocarbons by cracking. Although RHA also contains O-containing functional groups, they are insufficient due to the low S_{BET} for the conversion of N-species. Therefore, RHA could not promote denitrification. It is well known that the dehydration of amides can form nitriles (Kim et al., 2014). The decrease in the content of amides/amines and the increase in the content of nitriles indicated that the biochar catalyst enhanced the dehydration of amides/amines. RHC contains rich —COOH, O—C=O/—OH, and O—C=O/C—O groups with the highest S_{BET} (see Fig. 1 and Table 1), which promoted its nitrogen removal performance.

3.2.4. Effect of catalyst on the distribution of hydrocarbons in bio-oil

It is crucial to confirm the species and distribution of hydrocarbons in bio-oil. Therefore, hydrocarbons were divided into aliphatic, alicyclic, monocyclic aromatic, and polycyclic aromatic hydrocarbons in our study. The distributions of hydrocarbons are summarized in Fig. 2c for further analysis. Aliphatic hydrocarbons appear in the bio-oil after the addition of SWC, SRC, and RHC. This was mainly attributed to the cracking reaction of the long-chain substances (e.g. acids and amides/amines) that occurred on the biochar catalyst. Subsequently, part of the aliphatic hydrocarbons underwent cyclization to form alicyclic hydrocarbons, which corresponded to an increase in the content of alicyclic hydrocarbons. The contents of monocyclic aromatic hydrocarbons under the thermal, SWC, SRC, RHC and RHA catalyst were 15.57%, 30.87%, 33.39%, 40.22%, and 29.37%, respectively. It was observed that the content of monocyclic aromatic hydrocarbons increased sharply after introduction of catalyst, and RHC resulted in the highest content of monocyclic aromatic hydrocarbons. On the one hand, acid sites (e.g. —COOH) over catalyst promote the decarbonylation and oligomerization of furans to produce monocyclic aromatic hydrocarbons (Zhu et al., 2018), one the other hand, phenols removed side chains to generate monocyclic aromatic hydrocarbons. The introduction of RHA also increased the content of monocyclic aromatic hydrocarbons, which is probably due to the small number of O-containing groups on it to promote the formation of monocyclic aromatic hydrocarbons instead of nitrogen removal. The content of polycyclic aromatic hydrocarbons from the RHC catalyst decreased

Table 3
Ultimate analysis and properties of the bio-oil.

Sample	Co-pyrolysis	Thermal	SWC	SRC	RHC	RHA
Carbon (wt.%)	54.9	59.28	65.47	66.70	80.17	69.26
Hydrogen (wt.%)	7.8	7.57	9.23	7.40	6.35	6.58
Oxygen (wt.%)[a]	31.15	25.42	18.89	19.07	8.81	16.43
Nitrogen (wt.%)	5.85	7.3	6.40	6.42	4.38	7.16
Sulfur (wt.%)	0.30	0.43	0.01	0.41	0.29	0.57
HHV (MJ/kg)[b]	25.75	27.63	32.30	30.51	34.67	30.71
pH	4.06	4.34	5.32	5.27	5.48	5.01

[a] Determined by difference, O wt.%=100 - C wt.% - H wt.% - N wt.% - S wt.%.
[b] HHV (MJ/kg) = 34.1C + 123.9H − 9.85O + 6.3 N + 19.1 S (Xie et al., 2014).

greatly from 4.16% to 0.59% when compared to the thermal sample. It suggests that the formation of polycyclic aromatic hydrocarbons was significantly inhibited by RHC. (Wang et al., 2017b) reported similar results. Polycyclic aromatic hydrocarbons are precursors of carbon deposits, and the carbon deposits will greatly affect the catalyst activity. Therefore, low polycyclic aromatic hydrocarbons contents are conducive to improving the activity and lifetime of the catalyst.

In summary, RHC exhibited the best catalytic performance from the perspective of the increase in the content of hydrocarbons and decrease in the content of N-species. This is because it had the highest S_{BET}, which provides more opportunities for the reaction of pyrolysis intermediates with functional groups on the catalyst.

3.2.5. Effect of catalyst on the characteristics of bio-oil

The ultimate analysis results and properties of the bio-oil are summarized in Table 3. It was noticed that the bio-oil derived from co-pyrolysis had a pH value of 4.06, which means that bio-oil has high acidity and can increase the corrosion in downstream pipes and engine components. After the introduction of catalysts, the pH value (5.01–5.48) increased, which was attributed to the reductions in acids and phenols (see Fig. 2a) (Samanya et al., 2012). Besides, the oxygen content in catalytic bio-oil was lower than that of bio-oil obtained by co-pyrolysis, indicating that the catalytic co-pyrolysis has deoxygenation effect. The carbon content of the catalytic samples was higher than that of the co-pyrolysis sample, and the highest carbon content was achieved under RHC. This corresponded to the highest hydrocarbon contents that were achieved with the RHC in the above GC–MS result. Additionally, the HHV was significantly increased after catalytic co-pyrolysis, indicating that the quality of the bio-oil was significantly improved. Compared with the nitrogen content in co-pyrolysis bio-oil, nitrogen removal only occurred in RHC. This did not correspond to GC–MS results. This was probably due to the production of a large amount of large-molecular N-containing substances that cannot be detected by GC–MS after high-temperature catalysis, and the other biochar catalysts had little denitrification effect on such N-containing substances. A significant reduction in nitrogen content for liquid fuels is favorable, as high nitrogen contents may lead to environmental pollution issues. In summary, it was worth noting that the bio-oil of RHC exhibited the best deoxidation and denitrification effects, and possessed the highest calorific value and pH value. This was consistent with the GC/MS results.

3.2.6. Rice husk biochar deactivation experiment

Based on the chemical compositions and characteristics of the bio-oil discussed above, RHC exhibited the best catalytic performance. Therefore, we studied the deactivation experiment of RHC to investigate its activity. The RHC was used four times under the same experimental condition, and the products distribution and chemical composition of bio-oil are shown in Table A2 and Fig. 3, respectively. Table A2 indicates that the bio-oil yield

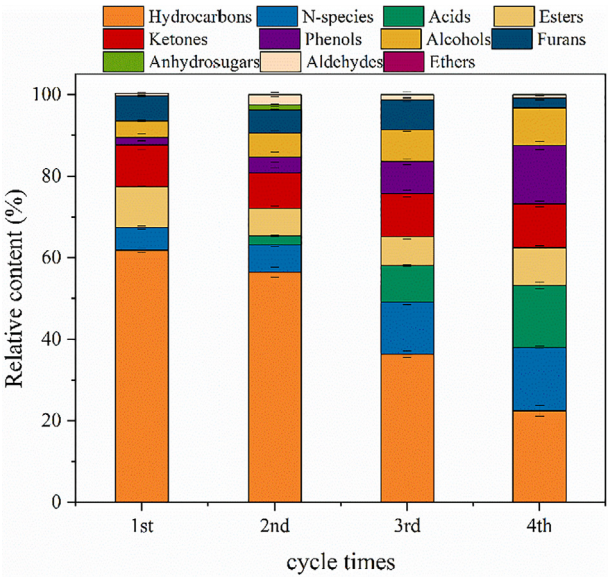

Fig. 3. Effect of catalyst recycling on the chemical composition of bio-oil.

increased with cycle times increasing, while the gas yield showed an opposite tendency. After the fourth use, the bio-oil yield (13.88 wt%) was close to that of the thermal sample (13.95 wt%). This may be due to two reasons: the catalytic performance of RHC was weakened; and carbon deposits on the RHC decomposed, then transformed into bio-oil. The content of hydrocarbons gradually decreased with the increase of cycle times, suggesting that the catalytic effect of RHC was decreased. The content of hydrocarbons (22.42%) decreased significantly, while those of N-species (15.59%), phenols (14.32%), and acids (15.21%) increased after four cycles. By comparing these results to the thermal sample (see Fig. 2a), the catalytic performance of RHC is lower than that of thermal reforming when it is used for the four times. Therefore, its catalytic activity can be guaranteed when used three times.

3.3. Catalytic co-pyrolysis mechanism of rice husk biochar

To further explore the catalytic mechanism of RHC, the characteristics of RHC after using are summarized in Table 4 and Fig. S4, and used RHC was denoted as U-RHC. The S_{BET} and D_a of U-RHC decreased to 40.87 m^2/g and 4.43 nm, respectively. The XPS analysis results indicate that the relative content of C-C in U-RHC was significantly increased, which was attributed to the formation of carbon deposits, which was consistent with the decrease in S_{BET} and D_a. Carbon deposits was due to the condensation of some pyrolytic intermediates during the catalytic co-pyrolysis. Besides, it could be found that C═O, O—C═O/C—O and —COOH decreased

Table 4
Physicochemical properties of the spent RHC.

Porous characteristics				
Name	S_{BET} (m^2/g)	V_t (cm^3/g)	D_a (nm)	
U-RHC	40.87	0.0397	4.43	
XPS analysis				
C-groups	C—C	C—O	C=O	
U-RHC content (%)	82.64	9.90	7.46	
O-groups	C=O	O—C=O/—OH	O—C=O/C—O	COOH
U-RHC content (%)	12.74	43.65	36.38	7.22
N-groups	Pyridinic-N	Amine/amide-N	Pyrrolic-N	Quaternary-N
U-RHC content (%)	9.29	16.80	28.85	45.06

after using, while only O—C=O/—OH increased significantly. The increase in O—C=O/—OH may be due to the following reasons: (1) the other O-containing functional groups could catalyze the transformation of pyrolytic intermediates to form simple phenols, and some simple phenols may be retained on the catalyst (Omoriyekomwan et al., 2016); (2) the reaction between phenols and the other O-containing functional groups can promote the removal of —OH from phenolic side chains and bind to O-containing groups. This also corresponded to the previous results that the content of phenols in bio-oil decreased significantly after the addition of the RHC catalyst, while the content of monocyclic aromatic hydrocarbons increased significantly.

Amine/amide-N first appeared on the surface of U-RHC. Amide-N may be derived from the reaction between —COOH/O—C=O and N-containing intermediates (amines/amides or NH_3/NH_2*) (Chen et al., 2018a, 2018b), while the long-chain fatty acids from the pyrolytic intermediate reacted with NH_3/NH_2* to form macromolecular amides/amines that aggregated on the catalyst surface.

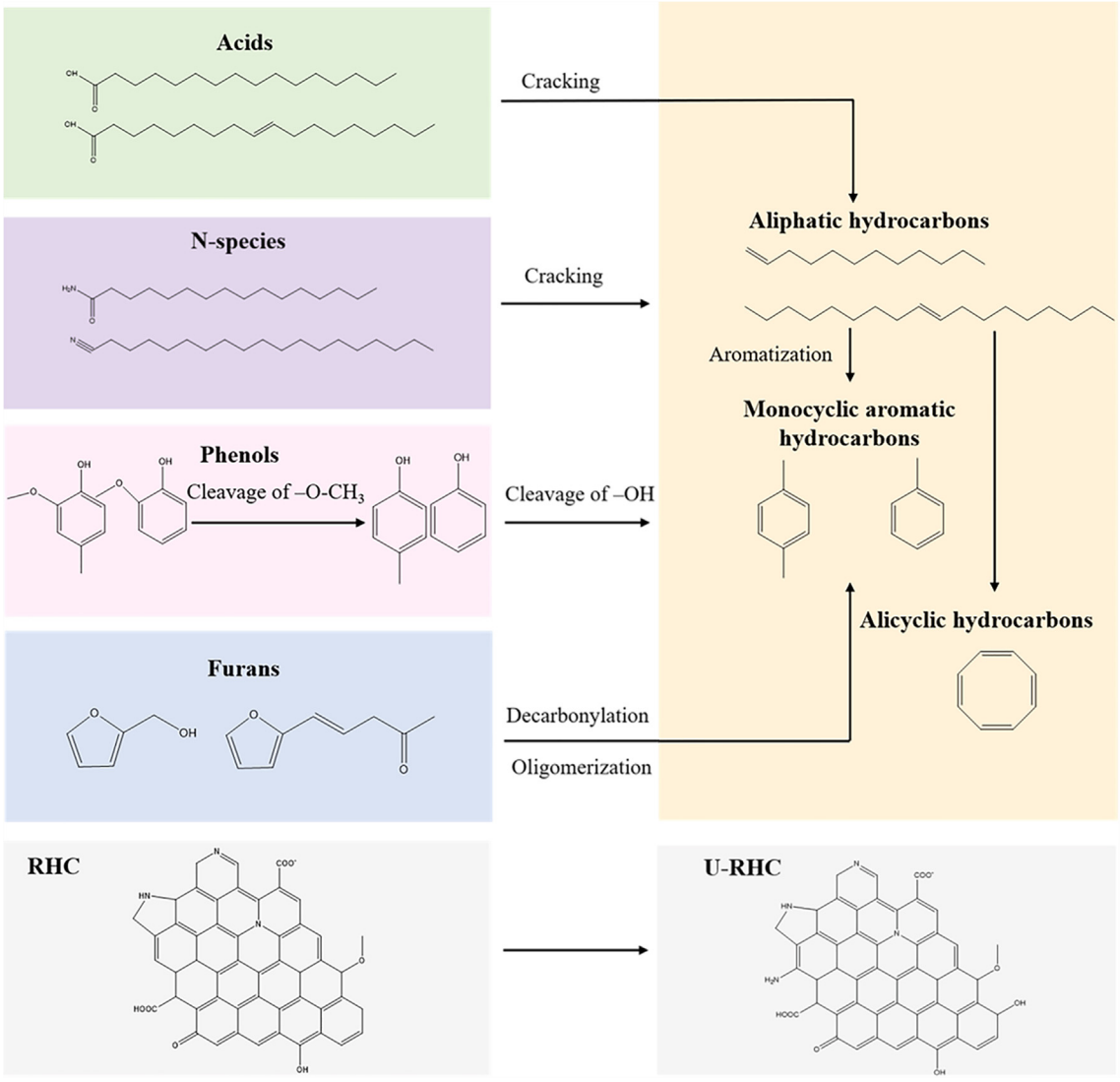

Fig. 4. Possible catalytic co-pyrolysis mechanism of RHC.

Pyridinic-N and pyrrolic-N could serve as active sites to catalyze the conversion of pyrolytic intermediates into phenols (Li et al., 2016). The substantial reduction in pyridine-N means that its catalytic activity of pyridine-N is stronger than that of pyrrole-N. Therefore, more phenols were formed, some of which remained on the catalyst, and some were further converted to form monocyclic aromatic hydrocarbons.

Based on the above analysis, the potential catalytic mechanism of RHC for the co-pyrolysis of SS and RH was determined and was presented in Fig. 4. During co-pyrolysis, large amounts of acids (e.g. n-hexadecanoic acid and oleic acid) and phenols (e.g. 3-methyl-phenol and 4-ethyl-phenol) were formed. Additionally, co-pyrolysis also produced some furans (e.g. *trans*-Furfurylideneacetone and 2-Furanmethanol) and large amounts of N-species (e.g. hexadecanamide and 3-methyl-Indole).

RHC acts as a catalyst during catalytic co-pyrolysis. Due to the rich pore structure of RHC, the pyrolytic intermediates fully reacted with the active N- and O-containing groups on the catalyst. As a result, the composition of bio-oil underwent tremendous changes. The content of hydrocarbons was significantly increased, while those of some long-chain substances (e.g. acids and amides/amines) and phenols were significantly reduced. The increase in the content of hydrocarbons was mainly due to three reasons. The first was that long-chain fatty acids and amides/amines underwent cracking to form aliphatic hydrocarbons, which could be further cyclized and aromatized into alicyclic and aromatic hydrocarbons. The second was the reduction in the content of phenols. Some studies have demonstrated that biochar catalysts contributed to the production of simple phenols by boosting the cleavage of —O—CH_3 (Yang et al., 2018), which are then converted into monocyclic aromatic hydrocarbons by the cleavage of —OH (Zhu et al., 2018). The increase in —OH and decrease in C═O, O—C═O/C—O, and —COOH over RHC suggest that simple phenols reacted with O-containing functional groups (e.g. C═O, O—C═O/C—O, and —COOH) over RHC to generate monocyclic aromatic hydrocarbons. Additionally, the —OH side chain was retained on RHC. Finally, the acid sites (e.g. —COOH) on RHC could promote the decarbonylation and oligomerization of furans, generating further aromatic hydrocarbons. Additionally, N-containing substances could not only crack to form hydrocarbons, but could also react with O-containing functional groups (e.g. —COOH, O—C═O) on the RHC, and remain on the catalyst in the form of amine/amide-N. This can be verified by the first appearance of amine/amide-N in U-RHC.

4. Conclusion

The effects of different catalysts on catalytic co-pyrolysis were investigated in a two-stage tube furnace. The GC–MS results demonstrated that biochar can promote the generation of hydrocarbons, while inhibiting the formation of O-containing (e.g. acids and phenols) and N-species (e.g. amides/amines and N-heterocyclics). The higher heating value and pH were also increased, thereby improving the quality of the bio-oil. RHC represented the best catalytic effects in terms of decreasing N-species by 58.79% and increasing hydrocarbons by nearly four times compared to co-pyrolysis. The increase in the content of hydrocarbons perhaps due to the cracking of long-chain substances, side-chain removal of phenols, and decarbonylation and oligomerization of furans. However, SRC did not show better catalytic performance than SWC and RHC, indicating that mixed biochar catalysts did not show the comprehensive advantages of SWC and RHC.

Declaration of Competing Interest

The authors declare that they have no known competing financial interests or personal relationships that could have appeared to influence the work reported in this paper.

Acknowledgements

This research was financially supported by a key research and development project of Hunan Province (2018WK2010, 2018WK2011), a project of the National Natural Science Foundation of China (No. 51679083), and the National Key Research Project, Ministry of Science and Technology of China (No. 2016YFF0204503-2).

Appendix A. Supplementary material

Supplementary data to this article can be found online at https://doi.org/10.1016/j.wasman.2020.07.013.

References

Alvarez, J., Amutio, M., Lopez, G., Bilbao, J., Olazar, M., 2015. Fast co-pyrolysis of sewage sludge and lignocellulosic biomass in a conical spouted bed reactor. Fuel 159, 810–818. https://doi.org/10.1016/j.fuel.2015.07.039.

An, Y., Tahmasebi, A., Zhao, X., Matamba, T., Yu, J., 2020. Catalytic reforming of palm kernel shell microwave pyrolysis vapors over iron-loaded activated carbon: Enhanced production of phenol and hydrogen. Bioresour. Technol. 306,. https://doi.org/10.1016/j.biortech.2020.123111 123111.

Arazo, R.O., Genuino, D.A.D., de Luna, M.D.G., Capareda, S.C., 2017. Bio-oil production from dry sewage sludge by fast pyrolysis in an electrically-heated fluidized bed reactor. Sustain. Environ. Res. 27, 7–14. https://doi.org/10.1016/j.serj.2016.11.010.

Ateş, F., Işikdağ, M.A., 2009. Influence of temperature and alumina catalyst on pyrolysis of corncob. Fuel 88, 1991–1997. https://doi.org/10.1016/j.fuel.2009.03.008.

Buentello-Montoya, D.A., Zhang, X., Li, J., 2019. The use of gasification solid products as catalysts for tar reforming. Renew. Sustain. Energy Rev. 107, 399–412. https://doi.org/10.1016/j.rser.2019.03.021.

Cai, W., Liu, R., He, Y., Chai, M., Cai, J., 2018. Bio-oil production from fast pyrolysis of rice husk in a commercial-scale plant with a downdraft circulating fluidized bed reactor. Fuel Process. Technol. 171, 308–317. https://doi.org/10.1016/j.fuproc.2017.12.001.

Carlson, T.R., Cheng, Y.-T., Jae, J., Huber, G.W., 2011. Production of green aromatics and olefins by catalytic fast pyrolysis of wood sawdust. Energy Environ. Sci. 4, 145–161. https://doi.org/10.1039/c0ee00341g.

Carlson, T.R., Jae, J., Lin, Y.-C., Tompsett, G.A., Huber, G.W., 2010. Catalytic fast pyrolysis of glucose with HZSM-5: The combined homogeneous and heterogeneous reactions. J. Catal. 270, 110–124. https://doi.org/10.1016/j.jcat.2009.12.013.

Chen, W., Fang, Y., Li, K., Chen, Z., Xia, M., Gong, M., Chen, Y., Yang, H., Tu, X., Chen, H., 2020. Bamboo wastes catalytic pyrolysis with N-doped biochar catalyst for phenols products. Appl. Energy 260. https://doi.org/10.1016/j.apenergy.2019.114242.

Chen, W., Li, K., Xia, M., Yang, H., Chen, Y., Chen, X., Che, Q., Chen, H., 2018a. Catalytic deoxygenation co-pyrolysis of bamboo wastes and microalgae with biochar catalyst. Energy 157, 472–482. https://doi.org/10.1016/j.energy.2018.05.149.

Chen, W., Yang, H., Chen, Y., Li, K., Xia, M., Chen, H., 2018b. Influence of Biochar Addition on Nitrogen Transformation during Copyrolysis of Algae and Lignocellulosic Biomass. Environ Sci Technol 52, 9514–9521. https://doi.org/10.1021/acs.est.8b02485.

Chen, W., Yang, H., Chen, Y., Xia, M., Chen, X., Chen, H., 2017. Transformation of Nitrogen and Evolution of N-Containing Species during Algae Pyrolysis. Environ Sci Technol 51, 6570–6579. https://doi.org/10.1021/acs.est.7b00434.

Daorattanachai, P., Laosiripojana, W., Laobuthee, A., Laosiripojana, N., 2018. Type of contribution: Research article catalytic activity of sewage sludge char supported Re-Ni bimetallic catalyst toward cracking/reforming of biomass tar. Renewable Energy 121, 644–651. https://doi.org/10.1016/j.renene.2018.01.096.

Dong, Q., Li, H., Niu, M., Luo, C., Zhang, J., Qi, B., Li, X., Zhong, W., 2018. Microwave pyrolysis of moso bamboo for syngas production and bio-oil upgrading over bamboo-based biochar catalyst. Bioresour Technol 266, 284–290. https://doi.org/10.1016/j.biortech.2018.06.104.

Duan, D., Zhang, Y., Lei, H., Villota, E., Ruan, R., 2019. Renewable jet-fuel range hydrocarbons production from co-pyrolysis of lignin and soapstock with the activated carbon catalyst. Waste Manage. 88, 1–9. https://doi.org/10.1016/j.wasman.2019.03.030.

Fonts, I., Gea, G., Azuara, M., Ábrego, J., Arauzo, J., 2012. Sewage sludge pyrolysis for liquid production: A review. Renew. Sustain. Energy Rev. 16, 2781–2805. https://doi.org/10.1016/j.rser.2012.02.070.

Fu, D., Li, X., Li, W., Feng, J., 2018. Catalytic upgrading of coal pyrolysis products over bio-char. Fuel Process. Technol. 176, 240–248. https://doi.org/10.1016/j.fuproc.2018.04.001.

Hu, Changsong, Zhang, Huiyan, Xiao, Rui, 2018. Effects of nascent char on ex-situ catalytic fast pyrolysis of wheat straw. Energy Conversion and Management. https://doi.org/10.1016/j.enconman.2018.10.018.

Kim, S.W., Koo, B.S., Lee, D.H., 2014. A comparative study of bio-oils from pyrolysis of microalgae and oil seed waste in a fluidized bed. Bioresour. Technol. 162, 96–102. https://doi.org/10.1016/j.biortech.2014.03.136.

Liu, X., Zhai, Y., Li, S., Wang, B., Wang, T., Liu, Y., Qiu, Z., Li, C., 2020. Hydrothermal carbonization of sewage sludge: Effect of feed-water pH on hydrochar's physicochemical properties, organic component and thermal behavior. J. Hazard. Mater. 388,. https://doi.org/10.1016/j.jhazmat.2020.122084 122084.

Li, M., Fan, X.u., Li, H., Wang, Y., 2016. Nitrogen-Doped Porous Carbon Materials: Promising Catalysts or Catalyst Supports for Heterogeneous Hydrogenation and Oxidation. Catal. Sci. Technol. 6, 3670–3693. https://doi.org/10.1039/x0xx00000x.

Naqvi, M., Yan, J., Dahlquist, E., Naqvi, S.R., 2016. Waste Biomass Gasification Based off-grid Electricity Generation: A Case Study in Pakistan. Energy Procedia 103, 406–412. https://doi.org/10.1016/j.egypro.2016.11.307.

Naqvi, S.R., Hameed, Z., Tariq, R., Taqvi, S.A., Ali, I., Niazi, M.B.K., Noor, T., Hussain, A., Iqbal, N., Shahbaz, M., 2019. Synergistic effect on co-pyrolysis of rice husk and sewage sludge by thermal behavior, kinetics, thermodynamic parameters and artificial neural network. Waste Manage. 85, 131–140. https://doi.org/10.1016/j.wasman.2018.12.031.

Norouzi, Omid, Jafarian, Sajedeh, Safari, Farid, Tavasoli, Ahmad, Nejati a, Behnam, 2016. Promotion of hydrogen-rich gas and phenolic-rich bio-oil production from green macroalgae Cladophora glomerata via pyrolysis over its bio-char. Bioresource Technology journal. https://doi.org/10.1016/j.biortech.2016.08.017 0960-8524/Ó.

Omoriyekomwan, J.E., Tahmasebi, A., Yu, J., 2016. Production of phenol-rich bio-oil during catalytic fixed-bed and microwave pyrolysis of palm kernel shell. Bioresour. Technol. 207, 188–196. https://doi.org/10.1016/j.biortech.2016.02.002.

Peng, C., Zhai, Y., Zhu, Y., Wang, Tengfei, Xu, B., Wang, Tao, Li, C., Zeng, G., 2017. Investigation of the structure and reaction pathway of char obtained from sewage sludge with biomass wastes, using hydrothermal treatment. J. Cleaner Prod. 166, 114–123. https://doi.org/10.1016/j.jclepro.2017.07.108.

Qiang, L., Wen-zhi, L., Dong, Z., Xi-feng, Z., 2009. Analytical pyrolysis–gas chromatography/mass spectrometry (Py–GC/MS) of sawdust with Al/SBA-15 catalysts. J. Anal. Appl. Pyrol. 84, 131–138. https://doi.org/10.1016/j.jaap.2009.01.002.

Ren, S., Lei, H., Wang, L., Bu, Q., Chen, S., Wu, J., 2014. Hydrocarbon and hydrogen-rich syngas production by biomass catalytic pyrolysis and bio-oil upgrading over biochar catalysts. RSC Adv. 4, 10731–10737. https://doi.org/10.1039/c4ra00122b.

Samanya, J., Hornung, A., Apfelbacher, A., Vale, P., 2012. Characteristics of the upper phase of bio-oil obtained from co-pyrolysis of sewage sludge with wood, rapeseed and straw. J. Anal. Appl. Pyrol. 94, 120–125. https://doi.org/10.1016/j.jaap.2011.11.017.

Shen, Y., Zhao, P., Shao, Q., Ma, D., Takahashi, F., Yoshikawa, K., 2014. In-situ catalytic conversion of tar using rice husk char-supported nickel-iron catalysts for biomass pyrolysis/gasification. Appl. Catal. B 152–153, 140–151. https://doi.org/10.1016/j.apcatb.2014.01.032.

Syed-Hassan, S.S.A., Wang, Y., Hu, S., Su, S., Xiang, J., 2017. Thermochemical processing of sewage sludge to energy and fuel: Fundamentals, challenges and considerations. Renew. Sustain. Energy Rev. 80, 888–913. https://doi.org/10.1016/j.rser.2017.05.262.

Tian, K., Liu, W.J., Qian, T.T., Jiang, H., Yu, H.Q., 2014. Investigation on the evolution of N-containing organic compounds during pyrolysis of sewage sludge. Environ Sci Technol 48, 10888–10896. https://doi.org/10.1021/es5022137.

Tsai, W.T., Lee, M.K., Chang, Y.M., 2007. Fast pyrolysis of rice husk: Product yields and compositions. Bioresour Technol 98, 22–28. https://doi.org/10.1016/j.biortech.2005.12.005.

Wang, T., Chen, Y., Li, J., Xue, Y., Liu, J., Mei, M., Hou, H., Chen, S., 2019. Co-pyrolysis behavior of sewage sludge and rice husk by TG-MS and residue analysis. J. Cleaner Prod. 119557. https://doi.org/10.1016/j.jclepro.2019.119557.

Wang, D., Chen, Z., Zhou, Z., Wang, Demin, Yu, J., Gao, S., 2019. Catalytic upgrading of volatiles from coal pyrolysis over sulfated carbon-based catalysts derived from waste red oil. Fuel Process. Technol. 189, 98–109. https://doi.org/10.1016/j.fuproc.2019.03.003.

Wang, J., Zhang, B., Zhong, Z., Ding, K., Deng, A., Min, M., Chen, P., Ruan, R., 2017a. Catalytic fast co-pyrolysis of bamboo residual and waste lubricating oil over an ex-situ dual catalytic beds of MgO and HZSM-5: Analytical PY-GC/MS study. Energy Convers. Manage. 139, 222–231. https://doi.org/10.1016/j.enconman.2017.02.047.

Wang, N., Chen, D., Arena, U., He, P., 2017b. Hot char-catalytic reforming of volatiles from MSW pyrolysis. Appl. Energy 191, 111–124. https://doi.org/10.1016/j.apenergy.2017.01.051.

Xie, Q., Peng, P., Liu, S., Min, M., Cheng, Y., Wan, Y., Li, Y., Lin, X., Liu, Y., Chen, P., Ruan, R., 2014. Fast microwave-assisted catalytic pyrolysis of sewage sludge for bio-oil production. Bioresour Technol 172, 162–168. https://doi.org/10.1016/j.biortech.2014.09.006.

Xu, X., Li, Z., Tu, R., Sun, Y., Jiang, E., 2018. Hydrogen from Rice Husk Pyrolysis Volatiles via Non-Noble Ni–Fe Catalysts Supported on Five Differently Treated Rice Husk Pyrolysis Carbon Supports. ACS Sustain. Chem. Eng. 6, 8325–8339. https://doi.org/10.1021/acssuschemeng.8b00343.

Yang, Z., Lei, H., Qian, K., Zhang, Y., Villota, E., 2018. Renewable bio-phenols from in situ and ex situ catalytic pyrolysis of Douglas fir pellet over biobased activated carbons. Sustain. Energy Fuels 2, 894–904. https://doi.org/10.1039/c7se00607a.

Yildiz, G., Ronsse, F., Venderbosch, R., van Duren, R., Kersten, S.R.A., Prins, W., 2015. Effect of biomass ash in catalytic fast pyrolysis of pine wood. Appl. Catal. B 168–169, 203–211. https://doi.org/10.1016/j.apcatb.2014.12.044.

Zhang, H., Shao, S., Xiao, R., Shen, D., Zeng, J., 2014a. Characterization of coke deposition in the catalytic fast pyrolysis of biomass derivates. Energy Fuels 28, 52–57. https://doi.org/10.1021/ef401458y.

Zhang, S., Dong, Q., Zhang, L., Xiong, Y., 2015. High quality syngas production from microwave pyrolysis of rice husk with char-supported metallic catalysts. Bioresour Technol 191, 17–23. https://doi.org/10.1016/j.biortech.2015.04.114.

Zhang, M., Resende, F.L.P., Moutsoglou, A., 2014b. Catalytic fast pyrolysis of aspen lignin via Py-GC/MS. Fuel 116, 358–369. https://doi.org/10.1016/j.fuel.2013.07.128.

Zhang, S., Su, Y., Ding, K., Zhu, S., Zhang, H., Liu, X., Xiong, Y., 2018. Effect of inorganic species on torrefaction process and product properties of rice husk. Bioresour Technol 265, 450–455. https://doi.org/10.1016/j.biortech.2018.06.042.

Zhang, Y.L., Wu, W.G., Zhao, S.H., Long, Y.F., Luo, Y.H., 2015. Experimental study on pyrolysis tar removal over rice straw char and inner pore structure evolution of char. Fuel Process. Technol. 134, 333–344. https://doi.org/10.1016/j.fuproc.2015.01.047.

Zhang, W., Yuan, C., Xu, J., Yang, X., 2015. Beneficial synergetic effect on gas production during co-pyrolysis of sewage sludge and biomass in a vacuum reactor. Bioresour Technol 183, 255–258. https://doi.org/10.1016/j.biortech.2015.01.113.

Zhao, H., Song, Q., Liu, S., Li, Y., Wang, X., Shu, X., 2018. Study on catalytic co-pyrolysis of physical mixture/staged pyrolysis characteristics of lignite and straw over an catalytic beds of char and its mechanism. Energy Convers. Manage. 161, 13–26. https://doi.org/10.1016/j.enconman.2018.01.083.

Zhou, J., Sui, Z., Zhu, J., Li, P., Chen, D., 2007. Characterization of surface oxygen complexes on carbon nanofibers by TPD, XPS and FT-IR. Carbon 45, 785–796. https://doi.org/10.1016/j.carbon.2006.11.019.

Zhu, L., Zhang, Y., Lei, H., Zhang, X., Wang, L., Bu, Q., Wei, Y., 2018. Production of hydrocarbons from biomass-derived biochar assisted microwave catalytic pyrolysis. Sustainable Energy Fuels 2, 1781–1790. https://doi.org/10.1039/c8se00096d.

Zuo, W., Jin, B., Huang, Y., Sun, Y., 2014. Characterization of top phase oil obtained from co-pyrolysis of sewage sludge and poplar sawdust. Environ. Sci. Pollut. Res. 21, 9717–9726. https://doi.org/10.1007/s11356-014-2887-7.